https://doi.org/10.5194/egusphere-2026-3317
Preprint. Discussion started: 2 July 2026

A Threshold-Based Method for Cloud Base Height Detection using Ceilometers: Application to Long-term observations in deriving Cloud Vertical Structure

Harshbardhan Kumar[1], V. Ravi Kiran[1], M. Venkat Ratnam[1], Herman Russchenberg[2], Arnoud Apituley[3]

[1]National Atmospheric Research Laboratory, Department of Space, Gadanki , 517 112, India.
[2]TU Delflt, Department of Geoscience and Remote Sensing, Delft, The Netherlands.
[3]Royal Netherlands Meteorological Institute (KNMI), Ministry of Infrastructure and Water management, Utrech, The Netherlands

Correspondence to: V. Ravi Kiran (ravikiranv@narl.gov.in)

Abstract. Ceilometers are widely used for cloud base height (CBH) detection, primarily through proprietary manufacturer algorithms. Although these algorithms are routinely employed at airports and meteorological stations, their suitability for climatological applications is often limited under complex atmospheric conditions. In this study, we propose an improved threshold-based detection (TBD) method for CBH retrieval that is applicable to both calibrated and non-calibrated ceilometer return signals. The detected cloud layers show good agreement with collocated observations from space-borne active sensors. A comparative analysis between the manufacturer's algorithm and the proposed TBD approach demonstrates significant improvement in CBH separation. The method is further shown to be adaptable to ceilometers of different makes operating under diverse environmental conditions. The TBD approach is applied to long-term observations (April 2020 – October 2025) from a CL51 ceilometer deployed in the coastal urban environment of Kolkata, eastern India, to investigate cloud processes and characterize cloud vertical structure. A parameter termed normalized cloud occurrence is estimated for single-, double-, triple-, and all-layer cloud cases to qualitatively examine cloud vertical distribution. The close similarity between the occurrence patterns of single-layer and all-layer clouds indicates the dominance of single-layer clouds over the study region, while multi-layer cloud occurrences provide additional insight into cloud vertical structure. Seasonal and diurnal analyses reveal the persistent presence of low-level clouds (< 2 km) throughout the day across all seasons. The CBH of low-level clouds gradually increases after 09:00 local time, peaks during 12:00–15:00, and subsequently decreases, likely driven by solar-heating-induced convection. Such convection facilitates vertical cloud development up to 8–12 km, depending on the season, except during winter. Additionally, a persistent elevated cloud layer near 4 km is observed, likely associated with temperature variations around the 0°C isotherm. The derived cloud vertical structure has important implications for understanding cloud radiative forcing and improving atmospheric model predictions.

Keywords: Ceilometer, Cloud base height, Threshold method, Coastal urban environment.

https://doi.org/10.5194/egusphere-2026-3317
Preprint. Discussion started: 2 July 2026

1. Introduction

Clouds cover nearly two-thirds of the Earth's surface and play a crucial role in maintaining planetary habitability by regulating temperature, driving the hydrological cycle, and influencing the climate system (Stephens, 2005; Bony et al., 2015). Despite their importance, limited understanding of the underlying physical processes governing clouds results in their poor representation in weather and climate models (Morrision et al., 2020). Consequently, clouds remain one of the primary sources of uncertainty in simulations of past climate and projections of future climate change (Voigt et al., 2021; Zelinka et al., 2022). In particular, knowledge of cloud vertical structure and cloud cover is essential for improving climate model performance (An et al., 2019). Identification of cloud layers within the atmosphere is also a critical (first) step in aerosol–cloud interaction studies (Ravi Kiran et al., 2022). Such information is equally important for practical applications, including aviation safety (Hopkin et al., 2019) and weather forecasting (Illingworth et al., 2015), where the presence and altitude of cloud layers directly influence operational decisions.

Cloud vertical structure can be observed using ground-based active remote sensing systems (lidar/radar), in situ measurements (radiosondes and balloon-borne cloud particle sensors), and satellite-borne active sensors (CloudSat/CALIPSO). In situ measurements, particularly those obtained from aircraft or UAVs, provide highly accurate observations of cloud structure; however, their application is limited by high operational costs, resulting in restricted spatial and temporal coverage. Balloon-borne in situ observations from radiosondes can also be used to infer cloud vertical structure and occurrence based on profiles of temperature and relative humidity (Zhang et al., 2018; Narendra Reddy et al., 2018; Xu et al., 2023). However, their relatively low temporal resolution (typically twice daily) and the drifting nature of balloons limit their ability to capture the temporal evolution of cloud fields. Satellite-borne active remote sensing systems provide global observations of cloud vertical structure (Bertrand et al., 2024); however, they suffer from sparse temporal sampling due to long revisit periods and provide only instantaneous snapshots because of their rapid overpass and narrow nadir-view geometry. While satellite-borne passive remote sensing systems do not provide information on cloud vertical structure. To bridge this observational gap, several ground-based cloud profiling networks have been established worldwide, providing continuous measurements with high temporal resolution.

Among ground-based instruments, ceilometers are the most widely used systems for determining cloud base height (CBH) (Costa-Surós et al., 2013; An et al., 2017; Maturilli and Ebell, 2018). Ceilometers are low-cost, single-wavelength, low-power automatic lidars that typically operate in the near-infrared wavelength range (~900–1064 nm). Since clouds are strong scatterers at these wavelengths, ceilometers do not require the high power and complexity associated with aerosol lidars (Hopkin E., 2019). Their operation is based on the lidar principle, in which a diode laser emits short pulses of light vertically into the atmosphere. These pulses are backscattered by air molecules, aerosols, and cloud particles, and the travel time of the returned signal is used to determine their corresponding altitudes. The cloud base is generally identified as the lowest altitude exhibiting enhanced backscatter due to increased particle concentration. Ceilometers can operate

https://doi.org/10.5194/egusphere-2026-3317
Preprint. Discussion started: 2 July 2026

continuously during both daytime and night-time conditions and are capable of detecting up to three cloud layers as per the manufacturers claim. However, during precipitation or fog events, the strongest backscatter signal may not originate from the actual cloud base. Therefore, processing algorithms must account for such cases to ensure accurate CBH detection.

Developed primarily for aviation applications, ceilometers provide essential real-time CBH information to support routine aircraft operations, particularly under low-visibility conditions (Werner et al., 2005). In recent years, improvements in instrument sensitivity and the expansion of ceilometer networks have significantly enhanced their utility for atmospheric research. Several regional observational networks, such as the E-PROFILE network within the European Meteorological Services Network (Haefele et al., 2016), the Cloudnet project under the Aerosol, Clouds and Trace Gases Research Infrastructure (ACTRIS; Morales et al., 2024), the Aerosol LiDAR Ceilometer Network (ALICENET; Bellini et al., 2024), the Iberian Ceilometer Network (ICENET; Cazorla et al., 2017), and the Automated Surface Observing System (ASOS) across the contiguous United States (An et al., 2017), are actively acquiring and disseminating vertical profiles of aerosols and cloud properties. Most of these regional networks employ centralized processing, quality control, and data harmonization frameworks to generate multiple value-added products in addition to those derived from manufacturer-provided algorithms.

Ceilometer-based CBH climatologies have also been reported for several regions across India, including Ahmedabad (Sharma et al., 2016; Vaishnav et al., 2019; Kamat et al., 2024), Pune (Naik et al., 2024), Mahabaleshwar (Leena et al., 2024), Thiruvananthapuram (Varikoden et al., 2011; Sumesh et al., 2021; Pramitha et al., 2026), Tirupati (Rao and Saikranthi, 2025), Hyderabad (Vanlalrochana et al., 2025), Leh–Ladakh (Shah et al., 2025), four airport sites across the Indo-Gangetic Plain (Shukla et al., 2026), Umiam, Shillong (Kundu et al., 2023), and Delhi (Arun et al., 2018; Latha et al., 2021). It is important to note that all these studies directly utilized CBH values reported by manufacturer algorithms, except Rao and Saikranthi (2025), who applied the Value Distribution Equalization (VDE) algorithm. This approach generates an equalized signal that enables consistent representation of signal magnitude from low- to high-level clouds, upon which thresholding can be applied for cloud-layer detection. Although manufacturer algorithms have proven reliable for operational applications, particularly in the aviation sector, certain limitations in their outputs were identified in the present study, which may affect their suitability for climatological investigations (see Section 2.3.4).

Previous studies have also reported discrepancies in manufacturer-derived CBH retrievals and, consequently, developed alternative CBH detection approaches. For example, Martucci et al. (2010) introduced a temporal height tracking (THT) algorithm for two co-located ceilometers (Vaisala CL31 and Jenoptik CHM15K) and demonstrated a significant improvement in the correlation between CBH estimates from the two instruments compared to their manufacturer-derived outputs. Similarly, Wang et al. (2018) compared CBH retrievals obtained using a non-standard instrumental method with those derived from the manufacturer's algorithm and found that the latter tends to overestimate CBH. Standard CBH detection algorithms are primarily designed to identify optically thick, liquid-containing clouds and often fail to detect

https://doi.org/10.5194/egusphere-2026-3317
Preprint. Discussion started: 2 July 2026

optically thin ice clouds. To address this limitation, Tricht et al. (2014) proposed the polar threshold (PT) algorithm, which is more sensitive to the optically thin hydrometeor layers commonly observed in polar regions. However, to the best of our knowledge, no single algorithm is universally applicable to all ceilometers; rather, their performance depends strongly on instrument characteristics and prevailing atmospheric conditions, necessitating case-by-case implementation.

In this context, we propose a threshold-based CBH detection approach that can be applied to both calibrated and non-calibrated ceilometer signals. The applicability of this method is further evaluated across different ceilometer makes and models. In addition, the method is applied to a long-term dataset (April 2020 to October 2025) from a measurement site in eastern India to establish a cloud vertical structure. The paper is organized as follows. Section 2 provides an overview of the observational site, briefly describes the ceilometer used in this study, and presents the detailed methodology for signal pre-processing and CBH detection under the relevant subsections. The results are discussed in Section 3, while Section 4 summarizes the key findings and outlines the future prospects of the study.

2. Data and methodology

2.1. Measurement site

A ceilometer was deployed at the Kolkata Camp Observatory of NARL (KCON) (Fig. 1), located at the Regional Remote Sensing Centre-East (RRSC-East) of ISRO, Kolkata. The measurement site represents a coastal urban environment situated at the interface between the outflow from the Indo-Gangetic Plain (IGP) and the inflow from the Bay of Bengal (BoB). The site is approximately 145 km from the Bay of Bengal and lies at an elevation of 5–10 m above mean sea level. The regional climatology is characterized by four distinct seasons: winter (December–February), pre-monsoon (March–May), monsoon (June–September), and post-monsoon (October–November). The background meteorological conditions of the measurement site are shown in Figure S1. Monthly mean climatological profiles of temperature (Fig. S1a) and relative humidity (Fig. S1b) are derived from radiosonde observations at the Kolkata/Dumdum station (22.65°N, 88.45°E), located approximately 23 km south of KCON. Rainfall records are obtained from the KCON's automatic weather station. Cloud fraction (Fig. S1c) plotted as a function of altitude (up to 18 km at 240 m vertical resolution) is derived from a gridded (2.5° × 2.5°) data product based on combined CloudSat and CALIPSO observations (Bertrand et al., 2024). For cloud fraction, the grid point nearest to the measurement site was selected to represent the regional climatological pattern. The uniqueness of the site is that it experiences presence of clouds and rain (Fig. S1d) during both the pre-monsoon and monsoon seasons. In particular, the clouds during the pre-monsoon are dark, rich in liquid water content, produce abrupt, heavy rains popularly known as Kalbaisakhi or norwesterlies (Raj et. al., 2025). On the other side monsoon clouds exists over the site with features specific to mesoscale cloud systems of Indian Summer Monsoon. Therefore the cloud features over Kolkata are specific to location and makes it an interesting site for study of cloud characteristics such as cloud base height.

https://doi.org/10.5194/egusphere-2026-3317
Preprint. Discussion started: 2 July 2026

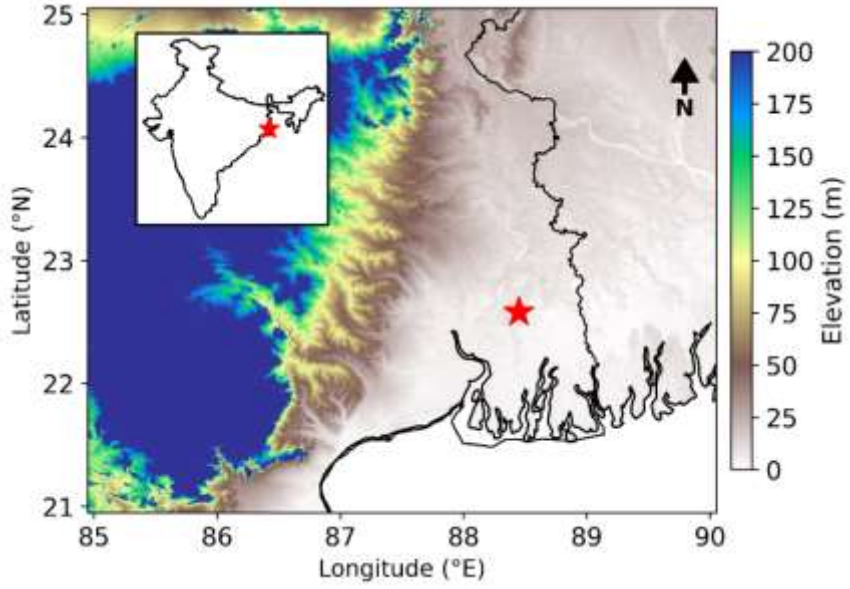

Figure 1. Geographical location of Kolkata Camp Observatory of NARL (KCON) (marked in red star: 22.58°N & 88.45°E) where the Vaisala CL51 ceilometer is operational since late March 2020.

2.2. Ceilometer

A Vaisala CL51 ceilometer was operational at RRSC-East, Kolkata, from late March 2020 onward. The CL51 utilizes an indium gallium arsenide (InGaAs) diode laser source that emits long-duration pulses of 110 ns centered at a wavelength of 910 ± 10 nm, with a repetition frequency of 6.5 kHz. The emitted pulses have a nominal energy of 3 μJ. The instrument design ensures eye-safe operation. The ceilometer records atmospheric backscatter signals up to an altitude of 15 km with a vertical resolution of 10 m. The on-board real-time data processing system generates three levels of output files that differ in terms of product type and resolution. Level-1 and Level-2 data files consists of range corrected signal (RCS), CBH processed through a pre-calculation stage and provide the full measurement range up to 15.4 km at 36 and 16 s temporal resolution respectively. Level-3 files include processed product variables derived from manufacturer-provided algorithms, such as mixing layer height and associated quality index parameters, up to an altitude of 4.5 km. In the present study, the Level-2 RCS data for the period April 2020 to October 2025 were utilized to derive CBH.

2.3. Pre-processing of Ceilometer return signal

Figure 2 presents an overview of the steps involved in ceilometer return-signal pre-processing up to CBH detection. Since the Level-2 ceilometer backscatter signals are reported in arbitrary units (a.u.), the RCS must be calibrated to derive the physical quantity, namely the total attenuated backscatter coefficient (m^{-1} sr^{-1}), prior to CBH detection. Before

https://doi.org/10.5194/egusphere-2026-3317
Preprint. Discussion started: 2 July 2026

calibration, however, it is essential to remove noise contributions arising from both atmospheric/solar background and instrument-related sources. According to the manufacturer, the on-board processing software estimates the receiver offset during each measurement cycle and applies a correction intended to account for the atmospheric background signal. Nevertheless, visual inspection of the profiles indicates that residual background contributions persist during both daytime and night time conditions, suggesting that additional noise correction is necessary. The following subsections (2.3.1 to 2.3.3) discuss the various processing steps illustrated in the flowchart below.

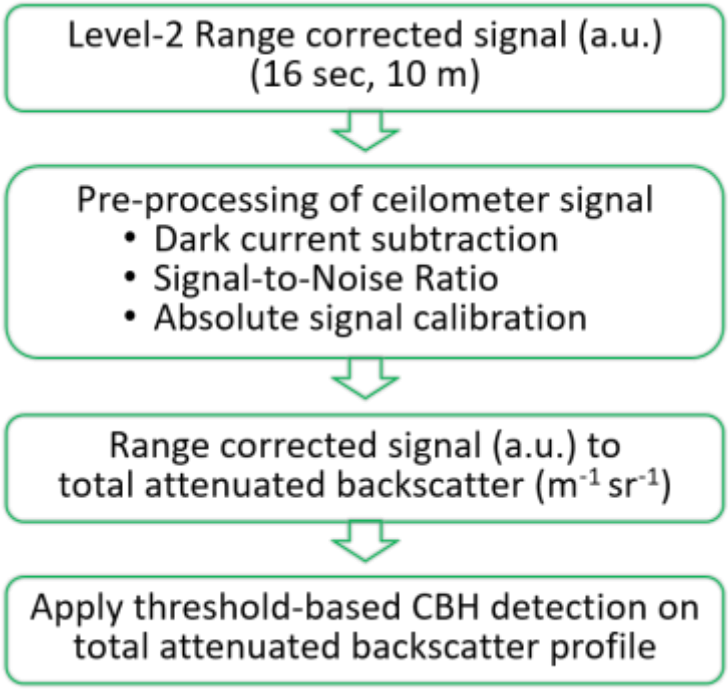

Figure 2. Flow chart showing the steps for ceilometer data pre-processing and cloud base height detection.

2.3.1. Instrument related background signal

The instrument-related background signal, also referred to as dark current, represents the cumulative background noise generated by the instrument's electronic and optical components, as well as by its internal data-processing system (Kotthaus et al., 2016). The standard approach for estimating and subtracting dark current in ceilometer measurements is the "termination hood" technique, in which a physical hood provided by the manufacturer completely attenuates the return signal, thereby allowing direct measurement of the instrument noise. In the absence of termination hood measurements, the dark current profile can be constructed from the total non-range-corrected signal (P) recorded by the ceilometer above a certain altitude under clear-sky conditions. Kotthaus et al. (2016) demonstrated that the median of hourly mean clear-sky midnight profiles (22:00–02:00 IST) shows good agreement with termination hood measurements for the Vaisala CL31

https://doi.org/10.5194/egusphere-2026-3317
Preprint. Discussion started: 2 July 2026

ceilometer. Following a similar approach, only range gates above 2000 m are utilized in the present study to estimate the dark current profile, thereby minimizing potential contributions from the atmospheric boundary layer. Over the study region, the boundary layer is typically confined below 2000 m (Basha et al., 2025). Below this altitude, a constant dark current value equal to that at 2000 m is assumed down to the surface.

At the present measurement site, clear-sky conditions during midnight hours are relatively less during most months, except in winter. Therefore, only profiles from November, December, and January were considered for constructing the dark current profile (Fig. S2). The median ± interquartile range of the time series of hourly mean clear-sky midnight P values, used for estimating the dark current, is shown in Figure 3 and represents the final dark current profile. This dark current profile was subsequently subtracted from each P profile to remove the instrument-related background contribution. The clear-sky profiles considered in this analysis are assumed to be aerosol free, although no complementary observations were available to verify this assumption. Finally, the range-corrected signal was derived from the dark-current-subtracted non-range-corrected signal.

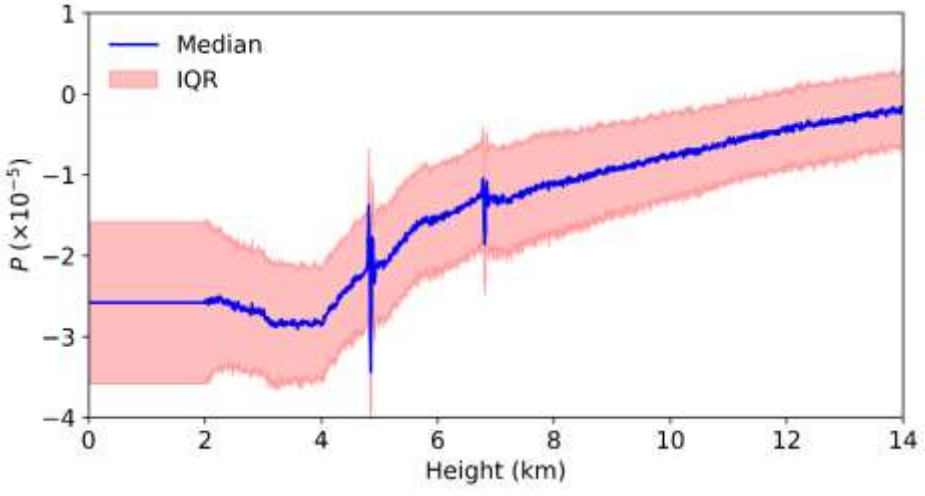

Figure 3. Median (solid blue) ± interquartile range (shaded pink) of 1023 hourly mean mid-night (22:00 to 02:00 IST) clear-sky non-range corrected signal (P) profiles.

2.3.2. Signal-to-Noise Ratio (SNR)

Inherent noise in recorded lidar returns primarily represents random signal fluctuations rather than meaningful atmospheric structures. Assuming that the signal at the farthest range gates is dominated by noise, the noise amplitude is estimated as the standard deviation of the uppermost 10% of the non-range-corrected signal bins from the top of the profile. The uppermost 10% of the profile (total bins, N = 154 at 10 m vertical resolution) is assumed to be sufficient to represent the variability in noise. The signal-to-noise ratio (SNR) is then computed by dividing the non-range-corrected signal by the

https://doi.org/10.5194/egusphere-2026-3317
Preprint. Discussion started: 2 July 2026

estimated noise amplitude. In general, an SNR greater than 1 indicates that the signal power exceeds the noise power. However, in ceilometer observations, significant contamination from daytime solar background radiation and night time random fluctuations persists for SNR values below 5. Therefore, a threshold of SNR > 5 is adopted in the present study to ensure robust atmospheric/solar background noise removal. This criterion is also consistent with the threshold used in the Cloudnet processing framework (Morales et al., 2024).

2.3.3. Absolute signal calibration

Absolute calibration is essential for ceilometer measurements, as it converts raw instrument-dependent signals into physically meaningful quantities, such as the attenuated backscatter coefficient, thereby enabling quantitative analysis and inter-comparison across different instruments. In ceilometers, an internal calibration is generally applied using a manufacturer-provided calibration constant. This factory-supplied calibration factor remains valid as long as the system efficiency and laser power are maintained at optimal levels. However, sensor performance degrades over time, necessitating periodic updates to the calibration factor. To address this issue, absolute calibration can be performed under well-characterized atmospheric conditions.

Within the lidar community, two widely used approaches for absolute calibration are the Rayleigh method, which relies on molecular backscatter from the upper atmosphere, and the cloud attenuation method, which utilizes the integrated backscatter from optically thick water clouds that fully extinguish the lidar beam (Hopkin et al., 2019). The Rayleigh method requires the identification of an aerosol-free region in the upper troposphere to establish the calibration reference. In practice, however, ceilometer signals often lack sufficient SNR in the upper troposphere to provide a reliable molecular return. Consequently, the stratocumulus cloud technique proposed by O'Connor et al. (2004) is considered more suitable for low-power ceilometers (Kotthaus et al., 2016). An important advantage of this approach is that it does not require supplementary observations from additional instruments.

When the ceilometer signal is fully attenuated within a cloud layer, the total path-integrated attenuated backscatter becomes equal to the reciprocal of twice the theoretical lidar ratio of a non-precipitating liquid cloud. Following the formulation presented by Marcos et al. (2018), the ceilometer signal integrated within a stratocumulus cloud layer can be approximated as follows:

$$\int_{\mathrm{base}}^{\mathrm{top}} \mathrm{RCS(r)dr} = \frac{\mathrm{C\,T_{base}^2}}{2\,\eta\,\mathrm{S}} \qquad (1)$$

Here, C is the calibration factor. T_{base}^2 represents the two-way transmittance between the ground and the cloud base, including contributions from molecules (T_{mol}^2), water vapor (T_{wv}^2), and aerosols (T_{aer}^2). **S** denotes the cloud lidar ratio,

https://doi.org/10.5194/egusphere-2026-3317
Preprint. Discussion started: 2 July 2026

defined as the ratio of extinction to backscatter, and is assumed to be constant (18.8±0.8 sr at 905 nm) for droplets in non-precipitating liquid water clouds (Hopkin et al., 2019; O'Connor et al., 2004).

The enhancement in backscatter and the apparent reduction in attenuation caused by multiple scattering are accounted for by introducing a multiple-scattering correction factor (η), which depends on the particle size distribution as well as the instrument beam divergence and receiver field of view. In the present study, the factor η was derived using the fitting coefficients reported by Marcos et al. (2018) for clouds with a droplet diameter of 8 μm and an extinction coefficient of 15 km^{-1} (Fig. S3). These coefficients were obtained from Monte Carlo simulations of multiply scattered lidar returns following the method of Kunkel and Weinman (1976). A third-degree polynomial fit was applied at every 10 m interval in cloud-base height between 500 and 3500 m to match the vertical resolution of the ceilometer observations. O'Connor et al. (2004) reported that, for beam divergences in the range of 1–1.5 mrad, multiple scattering can introduce an uncertainty of approximately 10% in the calibration. For the Vaisala CL51 ceilometer used in this study, the manufacturer specifies a transmitter beam divergence of ±0.15 mrad × ±0.25 mrad (https://docs.vaisala.com/r/M210801EN-K/en-US/GUID-9D1F1FD3-FEC1-4AC1-84DD-F4298DBB390D; last accessed on 9 April 2026). Based on these specifications, the uncertainty associated with multiple scattering is expected to remain below 10%.

The T^2_{mol} was estimated from molecular extinction profiles derived from radiosonde observations, whereas the T^2_{wv} was computed using the empirical relationship proposed in Equation 12 of Chen et al. (2025), based on hourly specific humidity profiles obtained from ERA5 reanalysis data. The ceilometer signal is attenuated by aerosol loading below the cloud layer, and this attenuation increases with aerosol concentration. In practice, completely aerosol-free profiles cannot be identified, particularly within the boundary layer. Therefore, cloud layers were manually selected such that the contribution from underlying background aerosols was minimal. An example of a suitable cloud layer used for calibration is shown in Figure 4. Furthermore, the T^2_{aer} below the cloud layer was determined iteratively following the procedure described by Marcos et al. (2018).

To apply this calibration technique, it is essential to select non-drizzling, liquid-phase cloud layers. In addition, low-altitude cloud layers should be avoided because of the possibility of incomplete overlap between the transmitted laser beam and the receiver field of view. Accordingly, cloud layers between 500 and 3000 m altitude, with a minimum thickness of 100 m, were selected for the analysis (Fig. S4). This selection criterion resulted in uneven sampling of profiles throughout the study period (Fig. S5). The time series of the final calibration factor (C) is presented in Figure S6. The total attenuated backscatter (TAB) profile ($m^{-1}sr^{-1}$ was obtained by dividing the dark-current- and background-noise-corrected range-corrected signal (RCS; a.u.) by the temporal mean calibration factor, $C = (1.50 \pm 0.37) \times 10^9$ m sr.

https://doi.org/10.5194/egusphere-2026-3317
Preprint. Discussion started: 2 July 2026

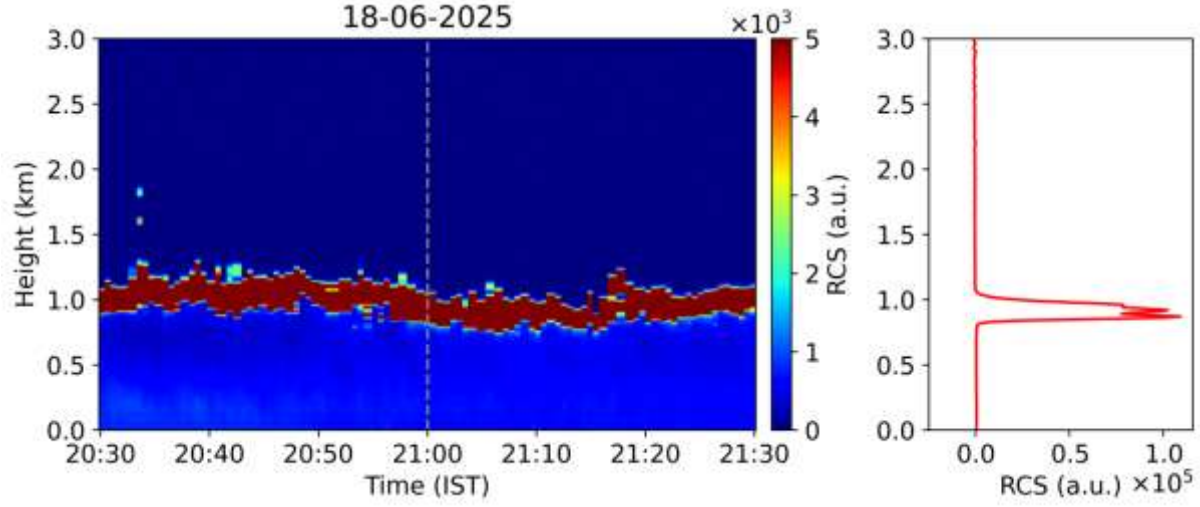

Figure 4. Illustrating the cloud attenuation method for estimation of ceilometer calibration factor using data recorded by ceilometer on 18 June 2025 over Kolkata.

2.3.4. Manufacture's algorithm (CL51) for CBH detection

While cloud base height (CBH) has previously been defined as the altitude at which the ceilometer signal attains its maximum value, such a definition often disagrees with pilot reports, which are primarily based on visibility conditions (Hopkin et al., 2019). Consequently, ceilometer manufacturers have developed proprietary algorithms for operational CBH detection. The Vaisala CL51 Sky Condition algorithm determines cloud-layer heights by analysing ceilometer measurements in both temporal and vertical dimensions. Detected cloud-base hits occurring at similar altitudes and within close temporal proximity are grouped into clusters, from which a representative height is calculated for each cluster. This representative height corresponds to the base height of the cloud layer associated with the cluster (https://docs.vaisala.com/r/M212735EN-A/en-US/GUID-79A170C6-2E42-4A7A-AC10-CD4E7F0CA4DD; last accessed on 9 April 2026). The proprietary operational algorithm provides CBH estimates in all three data levels (L1, L2, and L3).

However, a major limitation of the manufacturer's algorithm is that neither the algorithm itself nor the threshold parameters employed are publicly available or user-adjustable (Kotthaus et al., 2016). According to the instrument documentation, the algorithm is capable of simultaneously detecting up to three cloud layers. Although the manufacturer's algorithm has proven reliable for operational applications, particularly in the context of aviation safety, several limitations were identified in its output that may reduce its suitability for climatological studies. For example, the algorithm detects multiple cloud-base heights within the same physical cloud layer (Fig. 5), produces ambiguous CBH estimates during precipitation events (Fig. S7), and sometimes reports very low CBH values that are more likely associated with fog layers rather than actual cloud bases (Fig. S8). Most near-surface fog layers over the Indo-Gangetic Plain typically form within the

https://doi.org/10.5194/egusphere-2026-3317
Preprint. Discussion started: 2 July 2026

265 0–200 m altitude range (Arun et al., 2018; Ghude et al., 2023). In some cases, the clear-sky boundary-layer top is also identified as multiple cloud-base heights, particularly during the winter season (Fig. S9).

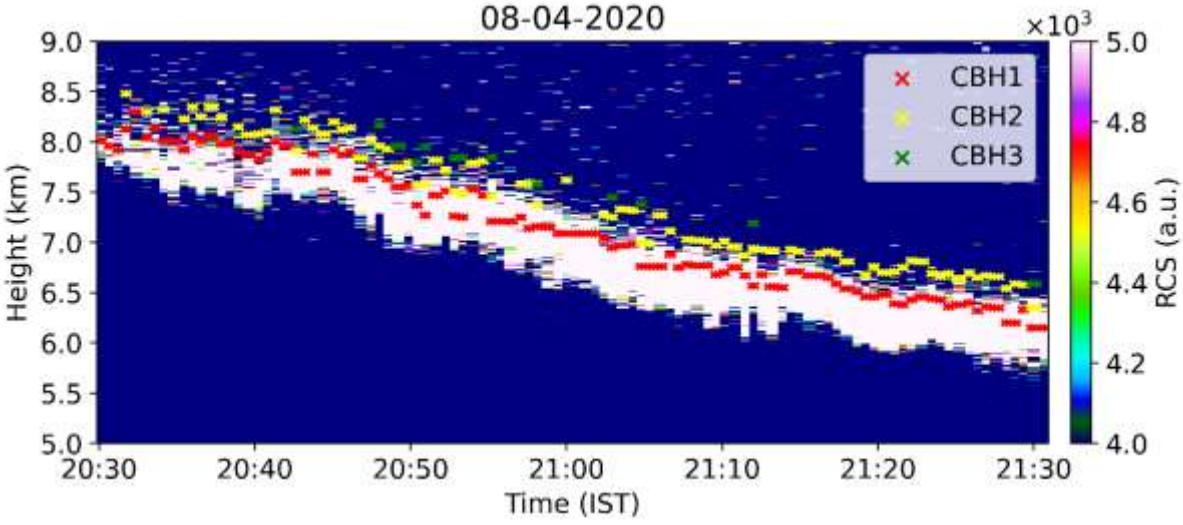

Figure 5. Example case showing the multiple CBH reported by CL51 algorithm in a single cloud layer.

270 **2.3.5. Threshold based detection (TBD) method**

Recognizing the limitations of the manufacturer's algorithm, a threshold-based CBH detection method has been developed. The threshold-based detection (TBD) method identifies CBH from vertical profiles of attenuated backscatter (ATB) or range-corrected signal (RCS) using predefined threshold values in combination with temporal and spatial consistency checks. The methodology is summarized as follows:

275 1. CBH is identified at the altitude where the ATB exceeds 1×10^{-5} ($m^{-1}sr^{-1}$). In the case of non-calibrated signals, CBH is identified where the RCS exceeds 1×10^{4} (a.u.).
2. The top of the layer (TOL) is defined as the altitude immediately above the detected CBH where the signal either drops to zero or becomes negative.
3. Only cloud layers with a thickness (TOL−CBH) of at least 50 m are retained in order to avoid pseudo-cloud layers
280 produced by random signal fluctuations.
4. To ensure temporal consistency, the CBH must be consistently detected in at least four consecutive profiles within a temporal window of (t±2), indicating the persistence of the layer for a minimum duration of approximately one minute.
5. To exclude slant precipitation streaks while still capturing gently descending cloud bases, the variation in CBH
285 across these consecutive profiles is restricted to within 200 m.
6. Profiles influenced by precipitation are excluded by identifying cloud layers with thicknesses greater than 1.5 km. This criterion was verified through visual inspection of several representative cases.

https://doi.org/10.5194/egusphere-2026-3317
Preprint. Discussion started: 2 July 2026

7. Fog cases are excluded by disregarding CBH detections below 200 m. Furthermore, CBH detections above 12 km are discarded because of poor signal-to-noise ratio (SNR) at higher altitudes.

An example comparison between CBH derived from the CL51 manufacturer algorithm and the TBD method is presented in Figure 6. The threshold-based method detected both single-layer and multi-layer cloud bases. The CBH overlaid as scatter points on the ATB profiles clearly indicate that the threshold-based method identified cloud bases at lower altitudes than CL51 algorithm. A discrepancy is also observed for one case in which the TBD method detected three CBH (220 m, 1150 m, and 1410 m), whereas the CL51 algorithm reported only two CBH (240 m and 1450 m).

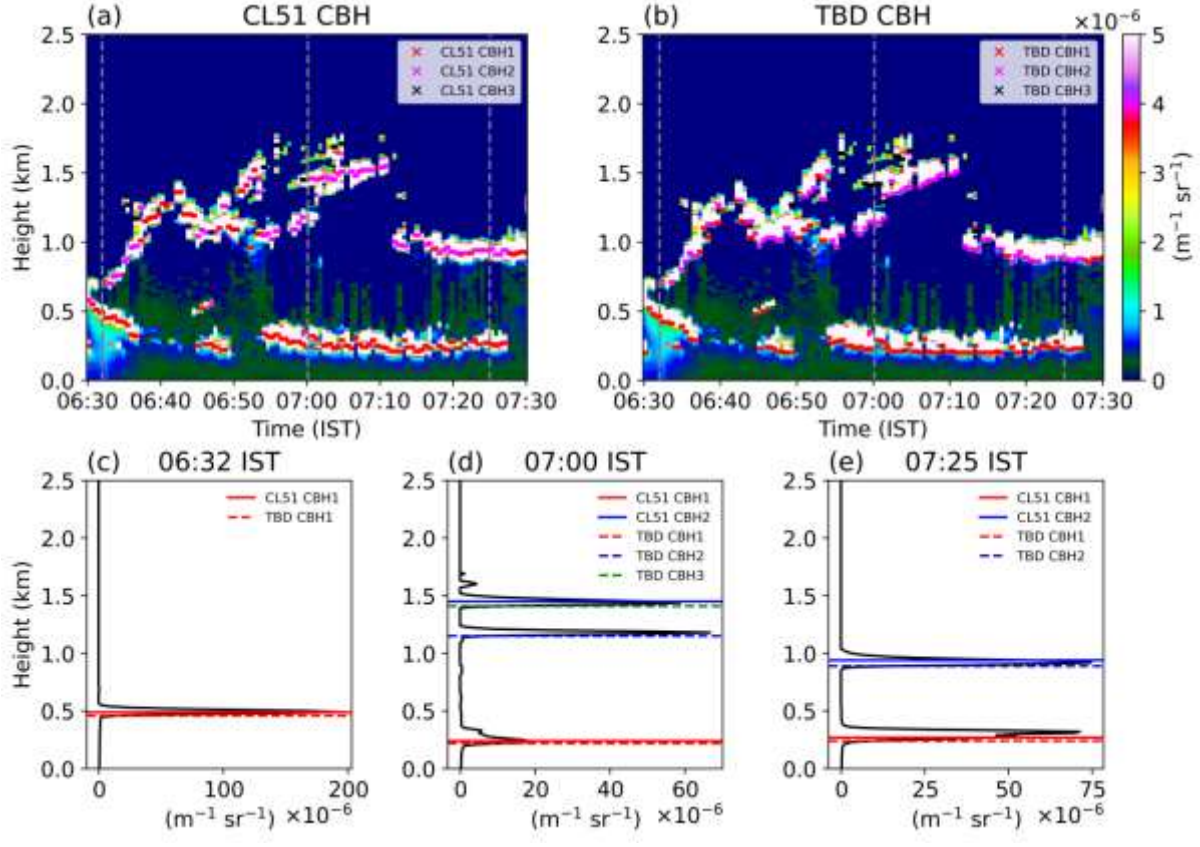

Figure 6. Example case illustrating the comparison of CBH detection using the CL51 algorithm and TBD method. The top panels show one-hour (06:30–07:30 IST) ATB profiles on 22 July 2024 overlaid with CBH as scatter from the CL51 and TBD methods. The bottom panels show three individual ATB profiles corresponding to the times marked by the grey dashed lines in the top curtain plots. Horizontal lines indicate the CBHs detected by both methods. For CL51 algorithm, CBH1, CBH2 and CBH3 are shown as solid lines, whereas for TBD method CBH are indicated by dashed lines in red, blue and green, respectively.

2.3.6. Comparison with space-borne observation

https://doi.org/10.5194/egusphere-2026-3317
Preprint. Discussion started: 2 July 2026

To inter-compare ground-based ceilometer measurements with satellite-based observations, lidar (CALIOP/CALIPSO) and radar (CPR/EarthCARE) observations falling within a ±0.25° box around KCON (22.58°N, 88.45°E) were selected. CALIOP/CALIPSO Level 1B profile data product (CAL_LID_L1-Standard-V5-00) is available on: https://search.earthdata.nasa.gov. CPR/EarthCARE data is available from European Space Agency, 2025, "EarthCARE CPR FMR Level 2A", (version AC), https://doi.org/10.57780/eca-d7a7dc9. Although, nearest match is recommended for comparison, due to non-availability of sufficient number of CALIPSO/EarthCARE overpasses, we have presented results for selective cases. A detailed study on inter-comparison will be taken up as a separate study. Figure 7 presents simultaneous cloud-layer observations over Kolkata obtained from the Cloud-Aerosol Lidar with Orthogonal Polarization (CALIOP) aboard the CALIPSO satellite and the ground-based CL51 ceilometer on 9 August 2020. The cloud base heights detected by the CL51 manufacturer algorithm, the TBD method, and CALIPSO were 2630 m, 2580 m, and 2837 m, respectively, demonstrating reasonably good agreement among the observations. A similar consistency is evident on 21 March 2023 for a cloud layer observed at higher altitudes between 8 and 10 km (Fig. S10).

Furthermore, Figure S11 illustrates the mapping of a thick precipitating cloud system by the Cloud Profiling Radar (CPR) aboard EarthCARE during an overpass directly above the ceilometer site on 21 June 2024. Within a one-hour period surrounding the CPR overpass, the ceilometer attenuated backscatter profiles exhibited intermittent cloud layers near 5 km when the transmitter–receiver window remained clear due to blower operation. However, when liquid water accumulated on the instrument window, complete signal attenuation was observed, thereby limiting cloud detection at higher altitudes. This inter-comparison demonstrates that the ceilometer provides reliable detection of non-precipitating cloud layers, whereas its performance is substantially degraded under precipitation conditions.

https://doi.org/10.5194/egusphere-2026-3317
Preprint. Discussion started: 2 July 2026

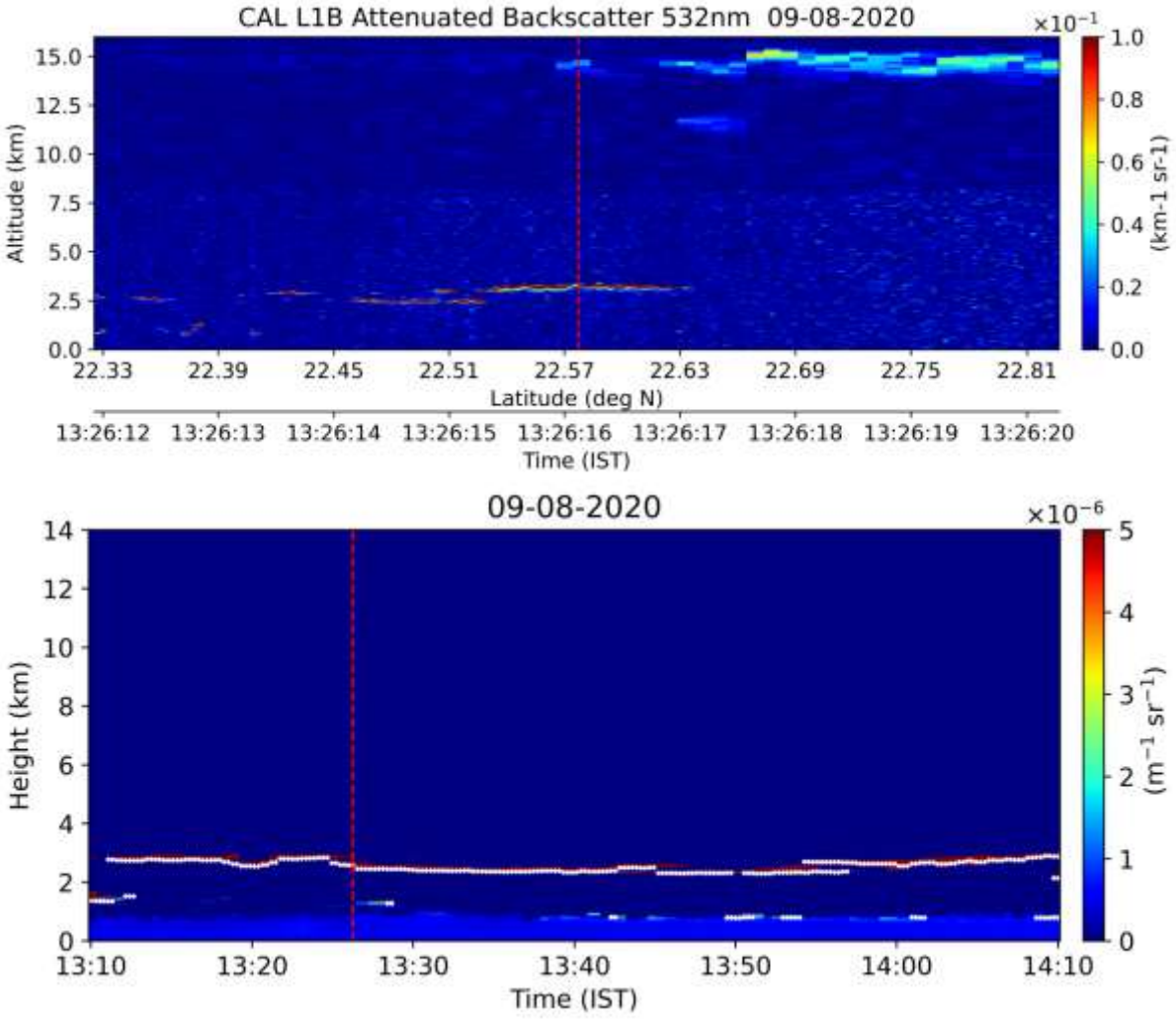

Figure 7. Concurrent observations of cloud layers on 9 August 2020 from a nearby night-time overpass of CALIOP/CALIPSO (top panel) and the CL51 ceilometer (bottom panel) at KCON measurement site. The red dashed line in the top panel indicates the CALIPSO track closest to the KCON site, while in the bottom panel it indicates the time of CALIPSO overpass. The cloud base heights detected by the CL51 algorithm, TBD method and CALIPSO are 2630 m, 2580 m, and 2837 m, respectively.

2.3.7. Applicability of TBD method

The TBD method described above was developed using data obtained from a Vaisala ceilometer. However, it is important to evaluate whether the method is also applicable to ceilometers from other manufacturers and deployed under different environmental conditions. To examine its broader applicability, the TBD method was tested using ceilometer datasets from the ACTRIS observational network, including different Vaisala models (CL61 operating at Lindenberg, Germany) as well as instruments from other manufacturers (Lufft CHM15k at Munich, Germany). In addition, data from a

https://doi.org/10.5194/egusphere-2026-3317
Preprint. Discussion started: 2 July 2026

Vaisala CL51 ceilometer located at Potenza, Italy, were also utilized. Ceilometer data within the ACTRIS network are collected, processed, and distributed through Cloudnet, which forms part of the ACTRIS research infrastructure maintained by the Finnish Meteorological Institute (https://docs.cloudnet.fmi.fi/; last accessed on 9 April 2026). For all three selected sites, signal-to-noise-ratio-filtered attenuated backscatter coefficient profiles were used as input to the TBD method for CBH detection.

For each site, representative comparisons between CBH derived from the manufacturer's algorithm and the TBD method are presented in Figure 8 and supplementary Figures S12 and S13. Across all example cases, a clear improvement in CBH detection is observed following the application of the TBD method. In particular, the TBD method largely avoids CBH detection during precipitation events and predominantly identifies single-layer clouds, in contrast to the multiple cloud layers frequently reported by the manufacturer's algorithm. These results demonstrate that the proposed method is robust across different ceilometer models and diverse observational environments.

https://doi.org/10.5194/egusphere-2026-3317
Preprint. Discussion started: 2 July 2026

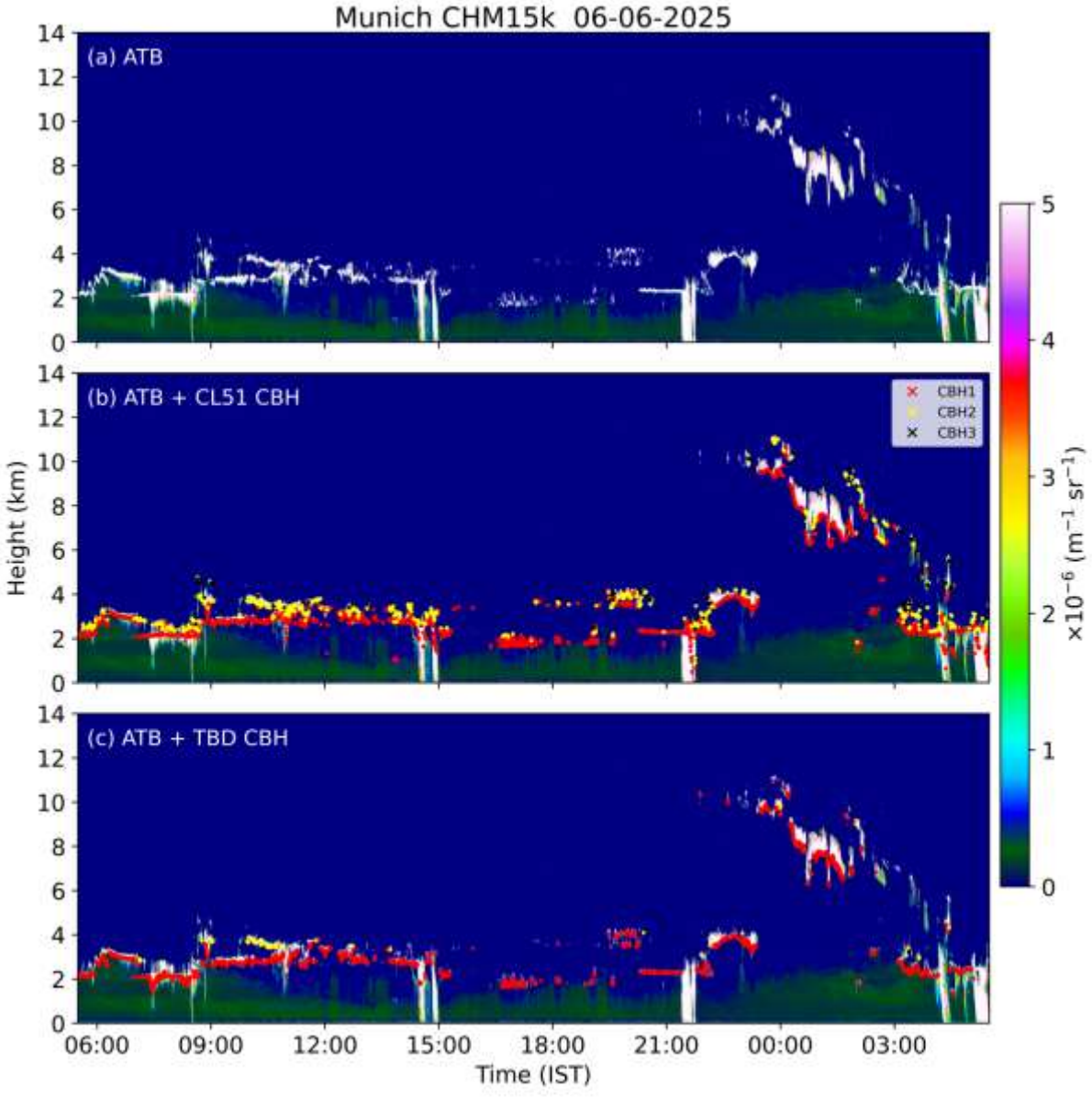

345 **Figure 8. (a) Attenuated backscatter profiles from Lufft CHM15k observations on 6 June 2025 at the ACTRIS site in Munich, Germany, overlaid with CBH detections shown as scatter points from (b) manufacturer's algorithm and (c) TBD method.**

2.3.8. Inter-comparison of methods

To quantify the differences in cloud-base-height (CBH) detection between the two methods, the separation between the first (CBH1) and second (CBH2) cloud layers was estimated. The monthly mean difference between CBH1 and CBH2 350 reveals a clear contrast between the TBD method and the CL51 manufacturer algorithm in resolving vertical layer separation (Fig. 9).

https://doi.org/10.5194/egusphere-2026-3317
Preprint. Discussion started: 2 July 2026

For the CL51 algorithm, the monthly mean difference exhibits an approximately bell-shaped seasonal pattern, with a maximum during the monsoon season (~1 km) and substantially smaller separations during winter (below 200 m). The standard deviation consistently exceeds the mean, indicating large variability throughout the year. In contrast, the TBD method shows significantly larger and more consistent CBH2–CBH1 separations across all months. The mean separation typically ranges from ~1–1.5 km during winter to ~2–3 km during the pre-monsoon and monsoon seasons, reflecting a more physically realistic vertical spacing between cloud layers. Furthermore, the standard deviation remains lower than the mean during most months, suggesting reduced variability and improved robustness in cloud-layer discrimination.

Previous studies over the Indian region using CBH values derived from manufacturer algorithms have also reported a large number of cases in which successive cloud bases are closely spaced. For example, Vanlalrochana et al. (2025) showed that, over the tropical urban site of Hyderabad, more than 50% of the cases across all seasons, the inter-CBH distance lies within 0–250 m, except during the monsoon season. Similarly, Kundu et al. (2023) found that 89.38% of cases exhibited a separation of less than 500 m between the first and second cloud layers at a remote hilly station in northeast India. Over western India, Vaishnav et al. (2019) also reported that the difference between CBH1 and CBH2 is typically below 500 m at Ahmedabad. Most of these studies further discussed the possible physical mechanisms responsible for such closely spaced CBH layers.

According to the manufacturer, ceilometers detect multilayer clouds by analysing the backscattered signal from laser pulses. However, when multiple CBHs are reported within close proximity inside a single cloud layer, attributing a clear physical interpretation becomes difficult without detailed knowledge of the underlying detection algorithm. One possible explanation is that a single broken or vertically inhomogeneous cloud layer passing through the ceilometer field of view may produce multiple backscatter peaks, thereby resulting in the detection of multiple cloud bases. To better address such cases, detection algorithms should incorporate a physically meaningful vertical separation threshold to distinguish genuinely separated cloud layers from fragments of the same layer. For example, cloud detection from radiosonde profiles often assumes that two contiguous layers belong to a single cloud layer if the vertical separation between them is less than 300 m (Reddy et al., 2018). Similarly, the International Satellite Cloud Climatology Project (ISCCP) reports that the global typical (average) separation between cloud layers is approximately 1 km (2 km) (https://isccp.giss.nasa.gov/analysis/wangpaper.html). Given these inherent limitations in ceilometer-derived multilayer detection, An et al. (2017) restricted their analysis to only the lowest cloud-base height when investigating the spatial and temporal variability of cloud occurrence across the contiguous United States.

https://doi.org/10.5194/egusphere-2026-3317
Preprint. Discussion started: 2 July 2026

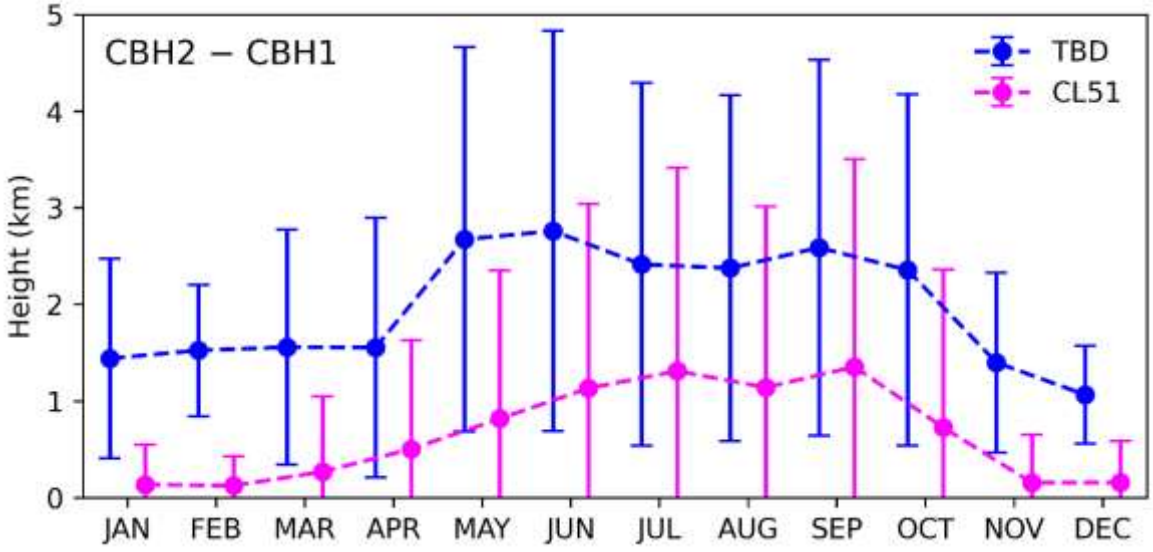

Figure 9. Monthly vertical separation between consecutive CBH detected by TBD method (blue) and CL51 algorithm (magenta) plotted as a function of month Error bar represents ± 1σ around.

3. Results and discussion

3.1. Cloud vertical structure

Long-term observations of total attenuated backscatter profiles obtained from the ceilometer have been utilized to establish the cloud vertical structure over Kolkata. In many previous studies, cloud vertical structure has been quantified using the frequency of cloud occurrence (expressed in percentage). However, due to the relatively smaller number of cloud-base heights detected by the TBD method (for the various reasons discussed above) the estimation of cloud occurrence frequency is not suitable for direct comparison. Alternatively, a qualitative approach has been adopted in which normalized cloud occurrence is estimated to simultaneously discuss the results from both the CL51 and TBD methods.

The instantaneous cloud-base heights detected by the two methods were first counted separately for every 250 m vertical bins. These cloud-base-count profiles were then normalized using min–max normalization for different temporal scales, including hourly and monthly periods, to represent the diurnal and seasonal variations in cloud vertical structure, respectively. In general, cloud occurrence decreases from single-layer to multilayer clouds, mainly because of the reduced ability of the laser beam to penetrate through lower cloud layers and detect elevated clouds (Costa-Surós et al., 2013). Even with enhanced laser power and improved detection sensitivity, the latest Vaisala model, CL61, still faces challenges in detecting upper-level clouds (Pramitha et al., 2026). Nevertheless, the cloud occurrences obtained at higher altitudes are sufficient to represent the presence of elevated cloud layers. A multilayer cloud vertical structure is expected over Kolkata. Therefore, the profiles were categorized into single-layer, two-layer, three-layer, and all-layer cloud cases, and normalized cloud occurrence was estimated separately for each category. Previous observations from space-borne active sensors indicate

https://doi.org/10.5194/egusphere-2026-3317
Preprint. Discussion started: 2 July 2026

that nearly 30% of low-level clouds are overlapped by higher cloud layers, with strong spatial variability exceeding 90% in tropical regions (Yuan et al., 2013).

Figure 10 illustrates the monthly variation in cloud vertical structure over Kolkata for all-layer clouds (Fig. 10a, e), single-layer clouds (Fig. 10b, f), two-layer clouds (Fig. 10c, g), and three-layer clouds (Fig. 10d, h), derived separately from the CL51 and TBD methods. Normalized cloud-occurrence values below approximately 0.05 were ignored and are therefore not shown in Figure 10. The highest normalized cloud occurrence, observed between 0 and 2 km for the all-layer cloud scenario (Fig. 10a, e) in both methods, indicates that low-level clouds predominate over Kolkata throughout the year. Importantly, the close similarity between the all-layer (Fig. 10a, e) and single-layer cloud distributions (Fig. 10b, f) suggests that single-layer clouds contribute predominantly to the cloud vertical structure over Kolkata.

It is also noteworthy that low-to-moderate normalized cloud occurrences are observed from approximately 2 km up to 8–10 km altitude from March through October, spanning the pre-monsoon, monsoon, and post-monsoon seasons. Such vertical cloud structures can be attributed to convective systems associated with Nor'westers during the pre-monsoon season (March–May), the southwest summer monsoon (June–September), and the northeast monsoon during October. However, the clear differences between the all-layer cloud structures shown in Figures 10a and 10e primarily arise from differences in cloud-base counts detected by the CL51 and TBD methods. In addition, the CL51 algorithm frequently reports multiple cloud-base heights within a single cloud layer with small vertical separations, as discussed in Section 2. The CL51 algorithm also detects multiple cloud bases during precipitation events and under near-surface fog conditions, thereby increasing the total number of detected cloud-base heights. In contrast, the TBD method avoids such cases and identifies cloud bases only for non-precipitating cloud conditions. Therefore, the CL51 results should be regarded as an inclusive representation of all atmospheric conditions, including precipitating and non-precipitating clouds, as well as fog and low-level cloud cases, whereas the TBD results represent only non-precipitating cloud layers over the measurement site.

The two-layer and three-layer cloud structures derived from the TBD method (Fig. 10g, h) reveal significant normalized cloud occurrence above 4 km, extending up to 8 km during the pre-monsoon season. Similar elevated cloud layers are also evident during the monsoon season (Fig. 10h), along with a strong presence of low-level cloud layers around 2 km (Fig. 10g). Furthermore, the cloud vertical structure during October, representing the post-monsoon season, indicates the presence of elevated cloud layers near 6 km. Elevated cloud layers observed during December are generally confined below 4 km. Collectively, the normalized cloud-occurrence features presented in Figures 10a–h indicate that the cloud vertical structure over Kolkata is characterized by persistent low-level clouds (below 2 km) throughout the year, together with elevated cloud layers extending up to 8 km from the pre-monsoon to the post-monsoon season.

https://doi.org/10.5194/egusphere-2026-3317
Preprint. Discussion started: 2 July 2026

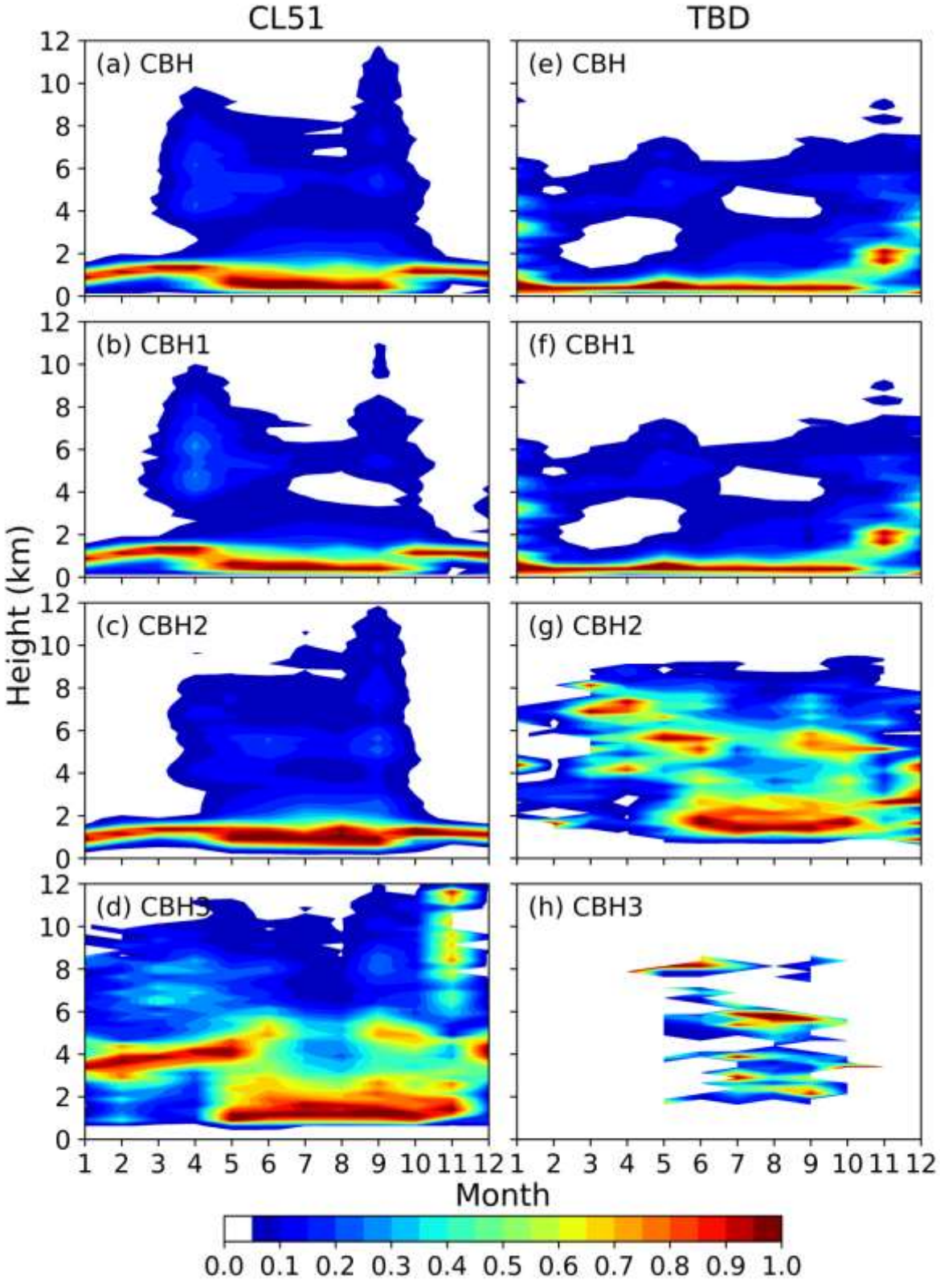

https://doi.org/10.5194/egusphere-2026-3317
Preprint. Discussion started: 2 July 2026

Figure 10. Monthly normalised occurrence of CBH obtained from CL51 algorithm and TBD method.

3.2. Diurnal variation in Cloud vertical structure

The diurnal variation of the seasonal mean cloud vertical structure over Kolkata derived from both methods is shown in Figure 11. The normalized cloud occurrence obtained from the CL51 algorithm is presented for all-layer clouds separately for the four seasons (Fig. 11a–d). Similarly, the normalized cloud occurrence derived from the TBD method is shown for single-layer clouds (Fig. 11e–h) and two-layer clouds (Fig.11i–l). The all-layer cloud occurrence derived from the TBD method is not shown because it was found to be similar to the single-layer cloud occurrence. The single-, double-, and three-layer cloud occurrences derived from the CL51 algorithm are presented in Figure S14.

Based on the normalized cloud occurrence derived from the CL51 algorithm (Fig. 11a), Kolkata experiences a thick layer of low-level clouds (below 2 km) during the winter season, which likely obscures the detection of cloud layers aloft. The strong cloud occurrence below 2 km during this season may be associated with both persistent low-level clouds and foggy conditions. As mentioned earlier, the CL51 algorithm does not distinguish fog from clouds and therefore treats fog layers as cloud layers. In contrast, the TBD method also depicts significant normalized cloud occurrence below 1 km until around noon (12 h). Thereafter, the normalized cloud occurrence shifts to slightly higher altitudes, indicating that increased solar insolation and subsequent surface heating around midday promote the lifting and cooling of air parcels, leading to cloud formation. Interestingly, significant cloud occurrence is also evident at elevated altitudes around 4 km after 12 h. In fact, such elevated clouds are present even before noon, as indicated by the two-layer normalized cloud occurrence (Fig. 11i). The elevated cloud layer persists until late evening (~20 h), while the lower-level cloud occurrence (below 2 km) gradually decreases. The formation of these elevated cloud layers may be associated with the presence of freezing temperatures above 4 km, as the 0 °C isotherm over Kolkata is also located near this altitude (Fig. S1a).

The normalized cloud occurrence during the pre-monsoon season, derived from all-layer clouds using the CL51 algorithm (Fig. 11b) and from single-layer clouds using the TBD method (Fig. 11f), depicts the vertical development of clouds associated with convection, together with the persistent presence of low-level clouds. The low-level cloud-base heights gradually rise from around 09 h until 12–15 h and subsequently decrease sharply during the late afternoon and evening. Strong solar insolation, which is typically highest during the pre-monsoon season compared to other seasons, together with intense surface heating, not only leads to the lifting of low-level cloud bases (similar to winter conditions) but also triggers vigorous convection. As a result, clouds develop vertically from around 4 km to as high as 8 km or above toward the evening hours. Subsequently, the top height of the vertically developed clouds decreases toward morning. Nevertheless, cloud formation around 4 km persists, likely because this altitude corresponds to the melting layer or the 0 °C isotherm. The CloudSat/CALIPSO cloud fraction profiles also clearly indicate the vertical development of clouds from approximately 3 km to higher altitudes as the season progresses from March onward (Fig. S1c). Such vertically developed

https://doi.org/10.5194/egusphere-2026-3317
Preprint. Discussion started: 2 July 2026

clouds are capable of producing rainfall, as reflected in Figure S1d, where an average accumulated rainfall of approximately 200 mm is recorded during May over Kolkata.

The cloud vertical structure during the monsoon season over Kolkata, as depicted by the normalized cloud occurrence derived from both methods (Fig. 11c, g, and k), exhibits features similar to those observed during the pre-monsoon season. However, a striking characteristic of the monsoon season is the enhanced vertical development of clouds, with cloud tops frequently extending beyond 8 km. The strong convection during the monsoon season is primarily driven by large-scale synoptic processes rather than localized convection, thereby resulting in deeply developed cloud systems. Similar features are also clearly evident from the CloudSat/CALIPSO observations, which indicate cloud vertical development extending up to 12 km and above (Fig. S1c). The CloudSat/CALIPSO observations provide an improved representation of cloud-top structures from a satellite perspective. Combining satellite and ground-based information will provide detailed information. Additional cloud layers are also evident from the two-layer normalized cloud occurrence shown in Figure 11k. Such multi-layered cloud vertical structures contribute to the highest accumulated rainfall observed during the monsoon season (Fig. S1d).

The cloud-occurrence characteristics during the post-monsoon season are generally similar to those observed during the preceding seasons. The atmosphere over Kolkata remains humid during October, corresponding to the post-monsoon period (Fig. S1b). The convectively unstable and moisture-rich atmospheric conditions favour the vertical development of clouds capable of producing rainfall (Fig. S1d). However, the atmosphere becomes considerably drier by November, and consequently, the occurrence of vertically developed cloud systems decreases substantially (Fig. S1c) towards winter.

https://doi.org/10.5194/egusphere-2026-3317
Preprint. Discussion started: 2 July 2026

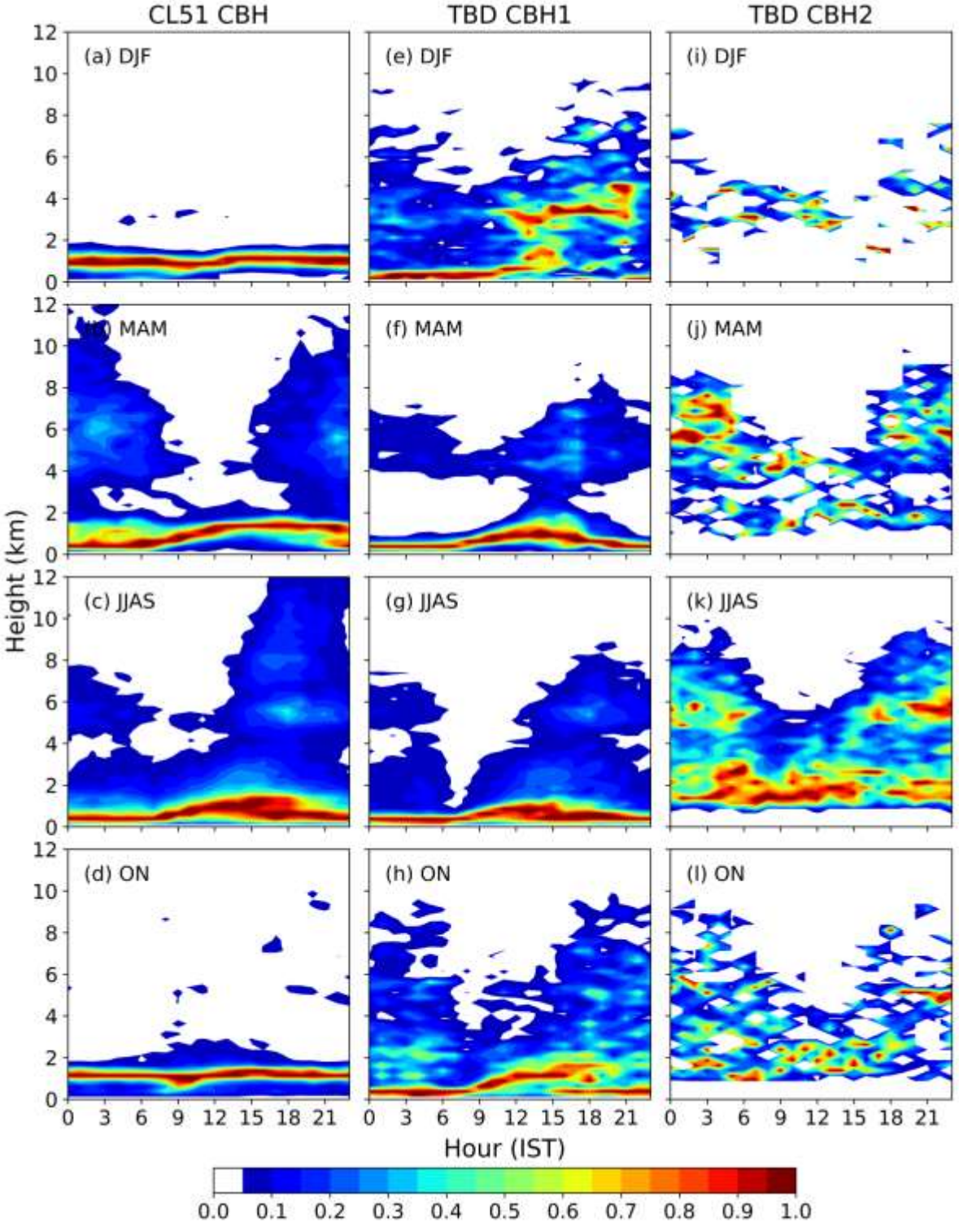

Figure 11. Season-wise hourly normalised cloud occurrence obtained from CL51 algorithm and TBD method.

https://doi.org/10.5194/egusphere-2026-3317
Preprint. Discussion started: 2 July 2026

4. Summary and Conclusions

Ceilometers are widely used for measuring cloud base height (CBH) because of their low cost, unattended day-and-night operation, and high temporal and vertical resolution. However, most studies rely directly on CBH derived from manufacturer-provided proprietary algorithms, which are primarily optimized for aviation applications, such as detecting the lowest cloud base for operational safety. Consequently, these algorithms are not always well suited for research applications, particularly climatological studies that require accurate detection of cloud layers.

To address this limitation, the present study introduces a threshold-based cloud base detection (TBD) method for CBH retrieval that can be applied to both calibrated and non-calibrated ceilometer signals. The raw ceilometer signals are first pre-processed to remove instrumental as well as atmospheric/solar background noise, and subsequently calibrated using the cloud-attenuation method to convert the range-corrected signal into a physically meaningful quantity, namely the total attenuated backscatter coefficient. The pre-processing steps adopted in this study are systematic and have not been implemented in the majority of previous studies. The CBH derived using the TBD method was compared using combined observations from CloudSat/CALIPSO and EarthCARE. In addition, the applicability of the TBD method was evaluated across ceilometers of different makes and models, demonstrating reliable and robust performance.

Furthermore, the TBD method was applied to long-term observations (April 2020 to October 2025) from a Vaisala CL51 ceilometer deployed at Kolkata (22.65°N, 88.45°E) in eastern India to establish the cloud vertical structure over the region. Our analysis indicates that the CL51 manufacturer algorithm tends to detect multiple cloud-base heights within a single cloud layer and frequently reports CBH under precipitating and foggy conditions. In contrast, the improved TBD method captures more distinct and physically realistic vertical separations between cloud layers under non-precipitating and non-foggy conditions. The manufacturer's algorithm predominantly reports closely spaced CBHs, particularly during the winter and post-monsoon seasons, whereas the threshold-based method identifies more clearly separated cloud layers. To facilitate comparison between the two methods, normalized cloud occurrence frequencies were estimated for single-layer, two-layer, three-layer, and combined (all-layer) cloud cases.

The similarity between the normalized cloud occurrences derived for all-layer and single-layer clouds suggests that single-layer clouds largely represent the cloud vertical structure over Kolkata. Low-level clouds (below 2 km) persist throughout the year irrespective of season. The cloud-base heights of these low-level clouds gradually increase during daytime, reaching their maximum values around noon, likely due to rising air parcels driven by enhanced solar insolation and associated surface heating. This convective activity becomes sufficiently strong to transport moist air upward, leading to the formation of vertically developed cloud systems after noon, extending up to approximately 8 km during the pre-monsoon season. The top heights of these vertically developed clouds subsequently decrease from midnight to early morning hours, often lowering to around 4 km. The dynamic pre-monsoon atmospheric conditions and associated vertically developed clouds are capable of producing sudden and intense rainfall events popularly known as Nor'westers.

https://doi.org/10.5194/egusphere-2026-3317
Preprint. Discussion started: 2 July 2026

During the monsoon season, cloud systems develop vertically from around 2 km to altitudes exceeding 12 km, reflecting strong synoptic-scale convection associated with the southwest monsoon in addition to local convective processes. Similarly, the vertical development of clouds observed during October, representing the post-monsoon season, is associated with the northeast monsoon along with local convection. Overall, vertically developed cloud systems are observed from March during the pre-monsoon season through October during the post-monsoon season, except during winter. Another important feature identified in this study is the persistent occurrence of elevated cloud layers near 4 km throughout the year, whose formation may be associated with the altitude of the 0 °C isotherm. Although the number of CBH detections for two-layer and three-layer cloud cases is comparatively smaller, the corresponding normalized cloud occurrence frequencies complement the single-layer cloud occurrence in representing the cloud vertical structure, including the vertical development of clouds. These features agree reasonably well with the cloud vertical structure derived from combined CloudSat/CALIPSO observations.

The present study demonstrates that ceilometer return signals, combined with CBH retrievals derived from the TBD method, not only improve the understanding of cloud processes but also provide a reliable representation of the cloud vertical structure specific to a given location. Such cloud vertical structure information can serve as a valuable input to radiative transfer models for investigating radiative transfer through clouds and estimating cloud radiative forcing at both the surface and the top of the atmosphere. In addition, this information can provide valuable constraints for numerical weather and climate models, thereby improving the representation of cloud vertical structure and enhancing prediction skill. Although the TBD method developed in this study demonstrates promising performance, the implementation of machine-learning-based approaches may provide a more robust solution, which constitutes a potential direction for future work.

Code and data availability

The code and data will be made available soon in public repository.

Author contributions

The contribution of the individual author is as follows. HK: Data curation, Formal analysis, Investigation, Methodology, Visualization, Original draft writing; VRK: Conceptualization, Methodology, Resources, Supervision, Original draft writing, Review and editing; MVR: Resources, Review and editing; HR: Review and editing; AP: Review and editing

https://doi.org/10.5194/egusphere-2026-3317
Preprint. Discussion started: 2 July 2026

Acknowledgements

The authors (HK, MVR, VRK) thank NARL for providing the necessary facilities to carry out this research. HK gratefully acknowledges financial support from the Anusandhan National Research Foundation (ANRF) under the National Post Doctoral Fellowship (NPDF) scheme [Grant No. PDF/2025/002285]. We acknowledge Aerosol, Clouds and Trace Gases Research Infrastructure (ACTRIS) and Finnish Meteorological Institute (FMI) for providing the Ceilometer dataset for Lindenberg and Munich (Germany) and Potenza (Italy) observational sites freely available online through Cloudnet. We also appreciate the CALIPSO, CloudSat and EarthCARE science teams for providing their dataset freely available online.

Competing interests

"The contact author has declared that none of the authors has any competing interests."

References

An, N., Pinker, R.T., Wang, K., Rogers, E. and Zuo, Z., 2019. Evaluation of cloud base height in the North American Regional Reanalysis using ceilometer observations.

An, N., Pinker, R.T., Wang, K., Rogers, E. and Zuo, Z., 2019. Evaluation of cloud base height in the North American Regional Reanalysis using ceilometer observations.

An, N., Wang, K., Zhou, C. and Pinker, R.T., 2017. Observed variability of cloud frequency and cloud-base height within 3600 m above the surface over the contiguous United States. Journal of Climate, 30(10), pp.3725-3742.

Arun, S.H., Sharma, S.K., Chaurasia, S., Vaishnav, R. and Kumar, R., 2018. Fog/low clouds detection over the Delhi Earth Station using the Ceilometer and the INSAT-3D/3DR satellite data. International Journal of Remote Sensing, 39(12), pp.4130-4144.

Basha, G., Ratnam, M.V. and Ravi Kiran, V., 2025. Quantification of urban region planetary boundary layer characteristics over edge of outflow of IGP and inflow of Bay of Bengal. Air Quality, Atmosphere & Health, 18(4), pp.1101-1113.

Bellini, A., Diémoz, H., Di Liberto, L., Gobbi, G.P., Bracci, A., Pasqualini, F. and Barnaba, F., 2024. ALICENET–an Italian network of automated lidar ceilometers for four-dimensional aerosol monitoring: infrastructure, data processing, and applications. Atmospheric Measurement Techniques, 17(20), pp.6119-6144.

Bertrand, L., Kay, J.E., Haynes, J. and de Boer, G., 2024. A global gridded dataset for cloud vertical structure from combined CloudSat and CALIPSO observations. Earth System Science Data, 16(3), pp.1301-1316.

Bony, S., Stevens, B., Frierson, D.M., Jakob, C., Kageyama, M., Pincus, R., Shepherd, T.G., Sherwood, S.C., Siebesma, A.P., Sobel, A.H. and Watanabe, M., 2015. Clouds, circulation and climate sensitivity. Nature Geoscience, 8(4), pp.261-268.

Cazorla, A., Casquero-Vera, J.A., Román, R., Guerrero-Rascado, J.L., Toledano, C., Cachorro, V.E., Orza, J.A.G., Cancillo, M.L., Serrano, A., Titos, G. and Pandolfi, M., 2017. Near-real-time processing of a ceilometer network assisted with sun-photometer data: monitoring a dust outbreak over the Iberian Peninsula. Atmospheric Chemistry and Physics, 17(19), pp.11861-11876.

Chen, J., Zeng, X., Li, S., Song, G. and Li, S., 2025. Water Vapor Correction in Measurements of Aerosol Backscatter Coefficients Using a 910 nm Vaisala CL51 Ceilometer. Remote Sensing, 17(12), p.2013.

https://doi.org/10.5194/egusphere-2026-3317
Preprint. Discussion started: 2 July 2026

Costa-Surós, M., Calbó, J., González, J.A. and Martin-Vide, J., 2013. Behavior of cloud base height from ceilometer measurements. Atmospheric Research, 127, pp.64-76.

Ghude, S.D., Jenamani, R.K., Kulkarni, R., Wagh, S., Dhangar, N.G., Parde, A.N., Acharja, P., Lonkar, P., Govardhan, G., Yadav, P. and Vispute, A., 2023. WiFEX: walk into the warm fog over Indo-Gangetic Plain region. Bulletin of the American Meteorological Society, 104(5), pp.E980-E1005.

Haefele, A., Hervo, M., Turp, M., Lampin, J.L., Haeffelin, M. and Lehmann, V., 2016, September. The E-PROFILE network for the operational measurement of wind and aerosol profiles over Europe. In Proceedings of WMO Technical Conference on Meteorological and Environmental Instruments and Methods of Observation, CIMO TECO.

Hopkin, E., 2019. Use of a calibrated ceilometer network to improve high resolution weather forecasts (Doctoral dissertation, University of Reading).

Hopkin, E., Illingworth, A.J., Charlton-Perez, C., Westbrook, C.D. and Ballard, S., 2019. A robust automated technique for operational calibration of ceilometers using the integrated backscatter from totally attenuating liquid clouds. Atmospheric Measurement Techniques, 12(7), pp.4131-4147.

Illingworth, A.J., Cimini, D., Gaffard, C., Haeffelin, M., Lehmann, V., Löhnert, U., O'Connor, E.J. and Ruffieux, D., 2015. Exploiting existing ground-based remote sensing networks to improve high-resolution weather forecasts. Bulletin of the American Meteorological Society, 96(12), pp.2107-2125.

Kamat, D.K., Sharma, S.K., Kumar, K.N., Kumar, P. and Saha, S., 2024. Cloud characteristics in the Aravalli ranges of Western India: insights from ground-based lidar measurements. Bulletin of Atmospheric Science and Technology, 5(1), p.11.

Kotthaus, S., O'Connor, E., Münkel, C., Charlton-Perez, C., Haeffelin, M., Gabey, A.M. and Grimmond, C.S.B., 2016. Recommendations for processing atmospheric attenuated backscatter profiles from Vaisala CL31 ceilometers. Atmospheric Measurement Techniques, 9(8), pp.3769-3791.

Kundu, A., Kundu, S.S., Sharma, S.K., Gogoi, M., Banik, T., Borgohain, A., Mahanta, R. and Debnath, A., 2023. The behavior of cloud base height over a hilly remote station of North-East India using ground-based remote sensing technique. Atmospheric Research, 282, p.106512.

Kunkel, K.E. and Weinman, J.A., 1976. Monte Carlo analysis of multiply scattered lidar returns. Journal of Atmospheric Sciences, 33(9), pp.1772-1781.

Latha, R., Murthy, B.S. and Sandeepan, B.S., 2021. Propagation of cloud base to higher levels during Covid-19-Lockdown. Science of the Total Environment, 759, p.144299.

Leena, P.P., Mise, D.J., Resmi, E.A., Anil Kumar, V., Chakravarty, K., Nirmin, K.S., Kumar, P.P., Patil, R.P. and Pandithurai, G., 2024. A statistical study on cloud base height behavior and cloud types during Southwest monsoon over a High-Altitude site in Western Ghats, India. Journal of the Indian Society of Remote Sensing, 52(1), pp.203-217.

Marcos, C.R., Gomez-Amo, J.L., Peris, C., Pedros, R., Utrillas, M.P. and Martinez-Lozano, J.A., 2018. Analysis of four years of ceilometer-derived aerosol backscatter profiles in a coastal site of the western Mediterranean. Atmospheric Research, 213, pp.331-345.

Martucci, G., Milroy, C. and O'Dowd, C.D., 2010. Detection of cloud-base height using Jenoptik CHM15K and Vaisala CL31 ceilometers. Journal of Atmospheric and Oceanic Technology, 27(2), pp.305-318.

Maturilli, M. and Ebell, K., 2018. Twenty-five years of cloud base height measurements by ceilometer in Ny-Ålesund, Svalbard. Earth System Science Data, 10(3), pp.1451-1456.

Morales, J.R., Calbo, J., Gonzalez, J.A. and Sola, Y., 2024. A method to assess the cloud-aerosol transition zone from ceilometer measurements. Atmospheric research, 310, p.107623.

Morrison, H., van Lier-Walqui, M., Fridlind, A.M., Grabowski, W.W., Harrington, J.Y., Hoose, C., Korolev, A., Kumjian, M.R., Milbrandt, J.A., Pawlowska, H. and Posselt, D.J., 2020. Confronting the challenge of modeling cloud and precipitation microphysics. Journal of advances in modeling earth systems, 12(8), p.e2019MS001689.

Naik, M., Jadhav, A.V., Mukhim, S., Pradeep Kumar, P. and Bhawar, R.L., 2024. Cloud base height variability observed using a Laser-Based Ceilometer over a tropical station Pune, India. International Journal of Remote Sensing, 45(22), pp.8441-8454.

https://doi.org/10.5194/egusphere-2026-3317
Preprint. Discussion started: 2 July 2026

Narendra Reddy, N., Venkat Ratnam, M., Basha, G. and Ravikiran, V., 2018. Cloud vertical structure over a tropical station obtained using long-term high-resolution radiosonde measurements. Atmospheric Chemistry and Physics, 18(16), pp.11709-11727.

O'Connor, E.J., Illingworth, A.J. and Hogan, R.J., 2004. A technique for autocalibration of cloud lidar. Journal of Atmospheric and Oceanic Technology, 21(5), pp.777-786.

Pramitha, M., Aathira, K.P. and Riya Raju, K., 2026. Seasonal variability of low, mid, and high level cloud properties over southern Western Ghats, India: a lidar ceilometer analysis. International Journal of Remote Sensing, 47(1), pp.266-287.

Raj, B., Sahoo, S., Puviarasan, N. and Chandrasekar, V., 2025. Diurnal Analysis of Nor'westers over Gangetic West Bengal as Observed from Weather Radar. Atmosphere, 16(8), p.989.

Rao, B.K. and Saikranthi, K., 2025. Impact of non-precipitating clouds on surface radiation components based on high-resolution in-situ data over a tropical station in southeast peninsular India. Science of The Total Environment, 1003, p.180659.

Shah, R., Sharma, S., Kamat, D., Kumar, K.N., Kumar, P., Ningombam, S.S., Angchuk, D. and Srivastava, R., 2025. Characteristics of multi-layer clouds observed using ceilometer observations over Leh-Ladakh: A high-altitude cold desert region. Atmospheric Research, p.108399.

Sharma, S., Vaishnav, R., Shukla, M.V., Kumar, P., Kumar, P., Thapliyal, P.K., Lal, S. and Acharya, Y.B., 2016. Evaluation of cloud base height measurements from Ceilometer CL31 and MODIS satellite over Ahmedabad, India. Atmospheric Measurement Techniques, 9(2), pp.711-719.

Shukla, K.K., Kumar, G., Mishra, A.K., Adhikary, S., Singh, N., Ranalkar, M.R., Sharma, R., Rai, M. and Shankar, A., 2026. Characteristic dissimilarities in the cloud base height over Indo-Gangetic plain airports during withdrawal phase of southwest monsoon. Meteorology and Atmospheric Physics, 138(1), p.9.

Stephens, G.L., 2005. Cloud feedbacks in the climate system: A critical review. Journal of climate, 18(2), pp.237-273.

Sumesh, R.K., Resmi, E.A., Unnikrishnan, C.K., Jash, D. and Ramachandran, K.K., 2021. Signatures of shallow and deep clouds inferred from precipitation microphysics over windward side of Western Ghats. Journal of Geophysical Research: Atmospheres, 126(10), p.e2020JD034312.

Vaishnav, R., Sharma, S., Shukla, K.K., Kumar, P. and Lal, S., 2019. A comprehensive statistical study of cloud base height using ceilometer over western India. Advances in Space Research, 63(5), pp.1708-1718.

Van Tricht, K., Gorodetskaya, I.V., Lhermitte, S., Turner, D.D., Schween, J.H. and Van Lipzig, N.P.M., 2014. An improved algorithm for polar cloud-base detection by ceilometer over the ice sheets. Atmospheric Measurement Techniques, 7(5), pp.1153-1167.

Vanlalrochana, H.Z., Rao, T.N., Jayachandran, V., Satheeshkumar, S. and Sudheesh, C., 2025. Characteristics of cloud base height distribution over a tropical urban region Hyderabad, India. Atmospheric Research, p.108476.

Varikoden, H., Harikumar, R., Vishnu, R., Sasi Kumar, V., Sampath, S., Murali Das, S. and Mohan Kumar, G., 2011. Observational study of cloud base height and its frequency over a tropical station, Thiruvananthapuram, using a ceilometer. International Journal of Remote Sensing, 32(23), pp.8505-8518.

Voigt, A., Albern, N., Ceppi, P., Grise, K., Li, Y. and Medeiros, B., 2021. Clouds, radiation, and atmospheric circulation in the present-day climate and under climate change. Wiley Interdisciplinary Reviews: Climate Change, 12(2), p.e694.

Wang, Y., Zhao, C., Dong, Z., Li, Z., Hu, S., Chen, T., Tao, F. and Wang, Y., 2018. Improved retrieval of cloud base heights from ceilometer using a non-standard instrument method. Atmospheric research, 202, pp.148-155.

Werner, C., Streicher, J., Leike, I. and Münkel, C., 2005. Visibility and cloud lidar. In Lidar: Range-Resolved Optical Remote Sensing of the Atmosphere (pp. 165-186). New York, NY: Springer New York.

Xu, H., Guo, J., Tong, B., Zhang, J., Chen, T., Guo, X., Zhang, J. and Chen, W., 2023. Characterizing the near-global cloud vertical structures over land using high-resolution radiosonde measurements. Atmospheric Chemistry and Physics, 23(23), pp.15011-15038.

Yuan, T. and Oreopoulos, L., 2013. On the global character of overlap between low and high clouds. Geophysical Research Letters, 40(19), pp.5320-5326.

Yusnaini, H., Marzuki, M., Hashiguchi, H., Ramadhan, R. and Saufina, E., 2025. Behavior of Cloud Base Height over Sumatra Mountains Region from Ceilometer Observations. Atmospheric Research, 317, p.107978.

https://doi.org/10.5194/egusphere-2026-3317
Preprint. Discussion started: 2 July 2026

Zelinka, M.D., Klein, S.A., Qin, Y. and Myers, T.A., 2022. Evaluating climate models' cloud feedbacks against expert judgment. Journal of Geophysical Research: Atmospheres, 127(2), p.e2021JD035198.

Zhang, Y., Zhang, L., Guo, J., Feng, J., Cao, L., Wang, Y., Zhou, Q., Li, L., Li, B., Xu, H. and Liu, L., 2018. Climatology of cloud-base height from long-term radiosonde measurements in China. Advances in Atmospheric Sciences, 35(2), pp.158-168.